# Quiet time ionospheric variability over Arecibo during sudden stratospheric warming events

J. L. Chau,[1] N. A. Aponte,[2] E. Cabassa,[2] M. P. Sulzer,[2] L. P. Goncharenko,[3] and S. A. González[2]

Received 18 February 2010; revised 7 April 2010; accepted 12 May 2010; published 11 September 2010.

[1] We present observations of the *F*-region ionosphere over Arecibo, Puerto Rico (18.34°N, 66.75°W), during the January–February 2008 and January–February 2009 sudden stratospheric warming (SSW) events. For the first period (2008), we have used incoherent scatter radar (ISR) electron density and temperature measurements from the Arecibo Observatory (AO), as well as relative total electron content (TEC) derived from a dual-frequency GPS receiver. For the second event (2009), during which we observed the largest recorded stratospheric warming, we have used the relative GPS TEC. Our analysis indicates that the ionosphere over Arecibo exhibits perturbations after the SSW, the effects are most visible during the daytime. The strongest signatures are observed in the TEC measurements, represented by large enhancements (with respect to non SSW days), particularly during daytime hours. However, the local time dependence of these enhancements is not the same in the two events. In addition, the data show that our results are consistent with the larger than normal daytime vertical drift differences observed at the magnetic equator over Jicamarca. The electron temperature is also affected during the daytime due to changes in electron density, indicating that the electron temperatures is influenced, indirectly, by changes in planetary wave activity in the lower altitudes.

**Citation:** Chau, J. L., N. A. Aponte, E. Cabassa, M. P. Sulzer, L. P. Goncharenko, and S. A. González (2010), Quiet time ionospheric variability over Arecibo during sudden stratospheric warming events, *J. Geophys. Res.*, *115*, A00G06, doi:10.1029/2010JA015378.

## 1. Introduction

[2] There is a very good understanding of the *F*-region ionosphere climatology, i.e., mean values for different seasons, solar conditions, and degrees of magnetic activity, as should be expected after more than 70 years of ionospheric observations. However, the understanding of its weather and thus our predictive capability, particularly during quiet and low solar flux conditions, is very poor. For example, it has long been recognized that there is large day-to-day variability in the vertical plasma drift observed at the magnetic equator, with this variability being the largest during solar minimum conditions [e.g., *Fejer et al.*, 1991; *Fejer and Scherliess*, 2001]. Similarly, changes of up to 20% in daytime *F*-region maximum electron density that cannot be associated with solar or magnetic drivers have been reported by *Rishbeth and Mendillo* [2001] and *Mendillo et al.* [2002]. These variations are comparable to ionospheric changes related to geomagnetic activity [e.g., *Fuller-Rowell et al.*, 2000; *Rishbeth and Mendillo*, 2001; *Forbes et al.*, 2000]. In the equatorial ionosphere, monthly ionospheric variability (i.e., monthly standard deviation over monthly mean) reaches 30–40% at sunrise and 15–30% at sunset [e.g., *Bilitza et al.*, 2004], while quiet time variations in daytime electron density can be as high as 200% [*Zhao et al.*, 2008]. This variability for many years has been thought to be associated with lower atmospheric forcing, e.g., planetary waves, tides, gravity waves, etc [e.g., *Richmond*, 1995; *Forbes et al.*, 2000; *Rishbeth*, 2006].

[3] Most of the previously reported ionospheric quiet time variability related to lower atmospheric forcing has been associated with similar wave/tide signatures observed in the lower atmosphere (quasi-16 day, two-day, tides, etc.). For example, *Forbes et al.* [2009] has reported evidence of tidal signatures at exospheric altitudes using satellite measurements. Early reports using single station observations were not as valuable as the new reports using a variety of instruments (including satellites) where the coupling is studied globally.

[4] At low latitudes and mid latitudes, the electrodynamic $\mathbf{E} \times \mathbf{B}$ equatorial plasma drifts, and in particular the vertical component, play important roles in the plasma distribution and dynamics. Due to the magnetic field geometry, there is

[1]Radio Observatorio de Jicamarca, Instituto Geofísico del Perú, Lima, Peru.
[2]Arecibo Observatory, Cornell University, National Astronomy and Ionosphere Center, Arecibo, Puerto Rico.
[3]Haystack Observatory, Massachusetts Institute of Technology, Westford, Massachusetts, USA.


0148-0227/10/2010JA015378

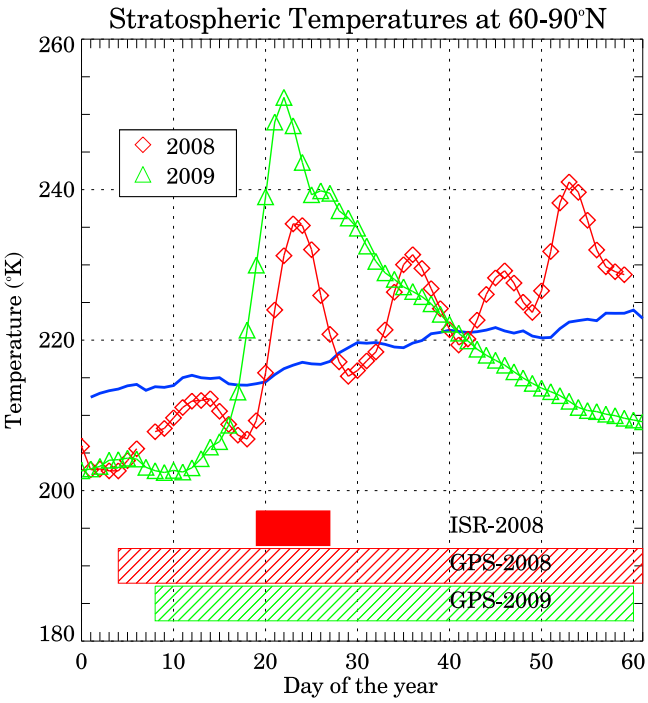


**Figure 1.** Stratospheric (10 hPa) temperatures at high latitudes (60–90°N) during the first two months of 2008 (red diamonds) and 2009 (green triangles). The horizontal bars indicate the times of ionospheric observations: ISR (solid) and GPS (hatched). The solid blue line represents the 30-year median value of the high latitude stratospheric temperature. Note the four sudden warming events in 2008 and one larger long lasting event in 2009.

an efficient fountain plasma transport process between the magnetic equator and the low and mid latitudes. An example of such efficiency is the generation of the equatorial ionization anomalies (EIAs) [*Hanson and Moffett*, 1966]. During quiet time periods, the equatorial plasma drifts result from the combined effects of *E* and *F* region magnetic field-line integrated thermospheric winds weighted by the integrated Pedersen conductivity [e.g., *Richmond*, 1995]. Using this simple representation, the equatorial ionospheric electrodynamics can be influenced by lower atmospheric forcing either directly via vertically-propagating tides/waves that modify the thermospheric winds and therefore the *F*-region dynamo, or indirectly via the *E*-region dynamo.

[5] At quiet times during the daytime, the *E*-region dynamo effects are stronger and electric field changes in the *E* region propagate efficiently to *F* region heights. This is because the wind pattern changes can more efficiently impose their signature. Moreover, during low solar conditions, the *F*-region dynamo is less efficient, allowing an easier (i.e., less confusing) identification of lower atmospheric forcing.

[6] Recently, *Chau et al.* [2009] have shown a strong correlation between anomalous equatorial plasma drifts and the occurrence of large meteorological events in the polar stratosphere. Such events, called sudden stratospheric warming (SSW), are characterized by dramatic variations at stratospheric altitudes at high latitudes. In a matter of few days, temperatures can increase by tens of Kelvins, the polar vortex can shift off the pole or split in two parts, and the zonal wind can change direction from westerly to easterly. The key mechanism for SSW events is the growth of planetary waves propagating upward from the troposphere and their non-linear interaction with the zonal mean flow [*Matsuno*, 1971].

[7] Both types of events, anomalous equatorial drifts and SSWs, appear to be caused by the same large scale planetary wave. In the case of the equatorial drifts, the planetary waves appear to interact nonlinearly with the atmospheric tides, which in turn modify the *E*-region winds and therefore the electric fields and plasma drifts of the *E*-region dynamo. This hypothesis is supported by a recent numerical modeling work [*Liu et al.*, 2010]. As mentioned above, for the daytime and low solar conditions, the dynamo effects easily modulate the ionospheric low latitude electrodynamics. Further evidence of this high-latitude stratosphere low-latitude ionosphere coupling has been also reported by *Vineeth et al.* [2009] and *Sridharan et al.* [2009]. Moreover, *Hysell et al.* [2009] have shown that during the daytime, the transition height $H^+$ to $O^+$, i.e., $h_t$, is highly correlated with the *E* region electric field (*F* region plasma drift), suggesting that lower atmospheric forcing could indirectly modulate the topside composition.

[8] But how is this coupling reproduced at other latitudes and longitudes? In this issue other colleagues [e.g., *Goncharenko et al.*, 2010b; *Fejer et al.*, 2010] are covering the same and other SSW events using a variety of instruments, and reporting effects at other longitudes and latitudes. In this work we concentrate in the ionospheric signatures above Arecibo observed during the January–February 2008 and January–February 2009 SSW events. We first present the main characteristics of the SSW events, then we show the electron density and temperature measurements performed with the Arecibo incoherent scatter radar (ISR) and the total electron content (TEC) from a GPS dual-frequency receiver. In addition we show the equatorial vertical drifts from Jicamarca (i.e., at the magnetic equator) to correlate such measurements with the Arecibo measurements. Finally we show and discuss that indeed the ionosphere over Arecibo is also affected during SSW events.

## 2. Sudden Stratospheric Warming Events

[9] The evolution of the stratospheric (10 hPa) polar temperatures for both the January–February 2008 (red, diamonds) and January–February 2009 (green, triangles) periods are shown in Figure 1. These data have been obtained from the National Center for Environmental Prediction (NCEP). The solid blue line represents a 30-year median value. The horizontal bars indicate the days with ionospheric observations (solid for ISR, hatched for GPS) over Arecibo.

[10] The January–February 2008 SSW event is one of the strongest recorded events but represents a minor warming because the zonal neutral wind (not shown here) reduced its magnitude but did not reverse sign. Note that after the initial warming, there were three more warming periods in the following weeks. The largest warmings were the first and fourth, respectively. On the other hand, the January–February

2009 event is the strongest and the longest lasting (more than three weeks) recorded event [e.g., *Manney et al.*, 2009]. This is considered a major warming event since the zonal neutral wind reversed sign.

[11] More details on the January 2008 event, the solar and magnetic indexes, and the ionospheric signatures observed at Millstone Hill and Jicamarca ISRs are given in the following seminal studies: *Goncharenko and Zhang* [2008] and *Chau et al.* [2009], respectively. Similarly, the details of the January–February 2009 SSW event, including other SSW parameters, are shown in other papers in this issue. In general, both periods were characterized by a very low solar flux (F10.7 < 80) and mostly quiet time conditions ($Kp < 3$).

## 3. Ionospheric Observations Over Arecibo and Jicamarca

[12] During January 2008 all the Incoherent Scatter Radars, including Arecibo and Jicamarca, operated almost continuously for nearly 10 days to observe the ionosphere effects, if any, of the January 2008 SSW event. In this work we are using the ISR data obtained with the Arecibo (AO) (18.34°N, 66.75°W) and Jicamarca (JRO) (11.95°, 76.8°W) ISRs. In the case of the JRO, located under the magnetic equator, we use the ISR vertical drift data. Details on the technique and the ISR experiment are given by *Chau et al.* [2009]. In the case of Arecibo, we are using the ISR data obtained from the plasma line portion of the experiment, i.e., daytime *F* region plasma densities and electron temperatures [e.g., *Nicolls et al.*, 2006]. The ISR parameters from the ion-line portion require additional analysis due to effects of receiver recovery and were not used in this study. Plasma line measurements were not affected.

[13] In addition to the ISR measurements, we are also using (a) the AO total electron content (TEC) obtained from the dual-frequency GPS receiver, and (b) the JRO daytime vertical drifts obtained from the 150-km echoes and the magnetometer ΔH (i.e., difference between the horizontal component of an equatorial station minus an off equatorial station). Relative TEC measurements have been obtained from combining the GPS received signals from both frequencies, and taking into account all the known errors and geometry. The procedure is very similar to the one described by *Rideout and Coster* [2006]. As indicated in Figure 1, we are only using ~50 days of data around the first peak of each event. Maps of similar TEC measurements, but all-over America, are presented and discussed by *Goncharenko et al.* [2010a]. The techniques for determining the JRO daytime vertical drifts using magnetometers and 150-km echoes are described by *Anderson et al.* [2004] and *Chau and Woodman* [2004], respectively. We are using the Jicamarca vertical drifts to help us in the interpretation of the results later.

### 3.1. Incoherent Scatter Radar Parameters

[14] In Figure 2 we show altitude-time maps of AO Electron densities ($\eta_e$) (Figure 2, left), AO Electron temperatures ($T_e$) (Figure 2, middle), and the JRO ISR vertical drifts (Figure 2, right), obtained few days around the January 2008 SSW event (i.e., January 19–26). Note that the plasma lines observations are only possible during the daytime. All of these observations are shown in Arecibo local time, i.e., AST. In all three plots, periods of no data are shown in white, and periods of bad data are shown in black.

[15] The main features that we observed in Figure 2 are:

[16] 1. There is a strong negative correlation between the AO $\eta_e$ and the AO $T_e$, i.e., when the electron density increases/decreases, the electron temperature decreases/increases. For example, at *F*-peak altitudes $T_e$ can go as low as 1000 K when $\eta_e$ is larger than $5 \times 10^5$ e/cm$^3$, while the electron temperature is larger than 2000 K for $\eta_e$ smaller than $\sim 2 \times 10^5$ e/cm$^3$.

[17] 2. Starting from January 21st, the JRO drifts start to present a clear semidiurnal signature. The amplitudes are stronger during the morning hours and they increase as time progresses. As reported by *Chau et al.* [2009], these semidiurnal waves with large amplitudes are highly correlated with stratospheric temperatures of the January 2008 SSW event (first warming).

[18] 3. The AO $\eta_e$ shows a clear and persistent double peak feature during the daytime, one early in the morning and the second one in the afternoon, particularly after January 20th.

[19] 4. There are apparent periodicities above the *F*-region peak in $\eta_e$ and $T_e$. These periodicities are due to: (1) the rotation of the Arecibo ISR beam, and (2) the presence of density gradients. The latter allows some beam positions to get signals at higher altitudes.

[20] To summarize the AO $\eta_e$ results, we have integrated in altitude the $\eta_e$ profile and obtained a proxy of TEC (TECp). In Figure 3, we show the TECp as function of time of the day (*y* axis) and day (*x* axis). The data gaps, indicated in black, represent either radar off periods or bad data (e.g., around 1000 LT on days 25 and 26). When the electron density is larger than the receiver bandwidth, the plasma line technique does not work. We are currently working on a method to fill these gaps of large $\eta_e$ with the ion-line portion of the experiment.

[21] From ISR TECp results, we can identify a region of TEC enhancement in the morning, starting around January 24–27, persisting for a few days and occurring later in time as the days progress. We also see other periods of enhancements (e.g., January 21), but these periods do not persist in time. Even though we are not including the topside electron density contribution, we believe the *F*-region densities we are using, are good proxies of the TEC behavior during this period [e.g., *MacPherson et al.*, 2000]. As we see later, the TEC obtained from GPS also show similar features. At this point, we can identify a weak signature that can be associated with the January SSW event, i.e., persistent TECp enhancement after January 24.

### 3.2. Arecibo Total Electron Content and Jicamarca Drifts

[22] In order to see if there are SSW effects over the Arecibo ionosphere with time scales similar to the SSW events, i.e., few days to weeks, we decided to analyze a longer time series, in this particular case, the relative total electron content (TEC) obtained from a GPS receiver. In Figure 4 we show the GPS TEC observations around the 2008 SSW events. Figure 4a shows the complete time series from early January until the end of February covering the four SSW events of 2008. In Figure 4b, we show the time series but as function of time of the day. In this plot we also

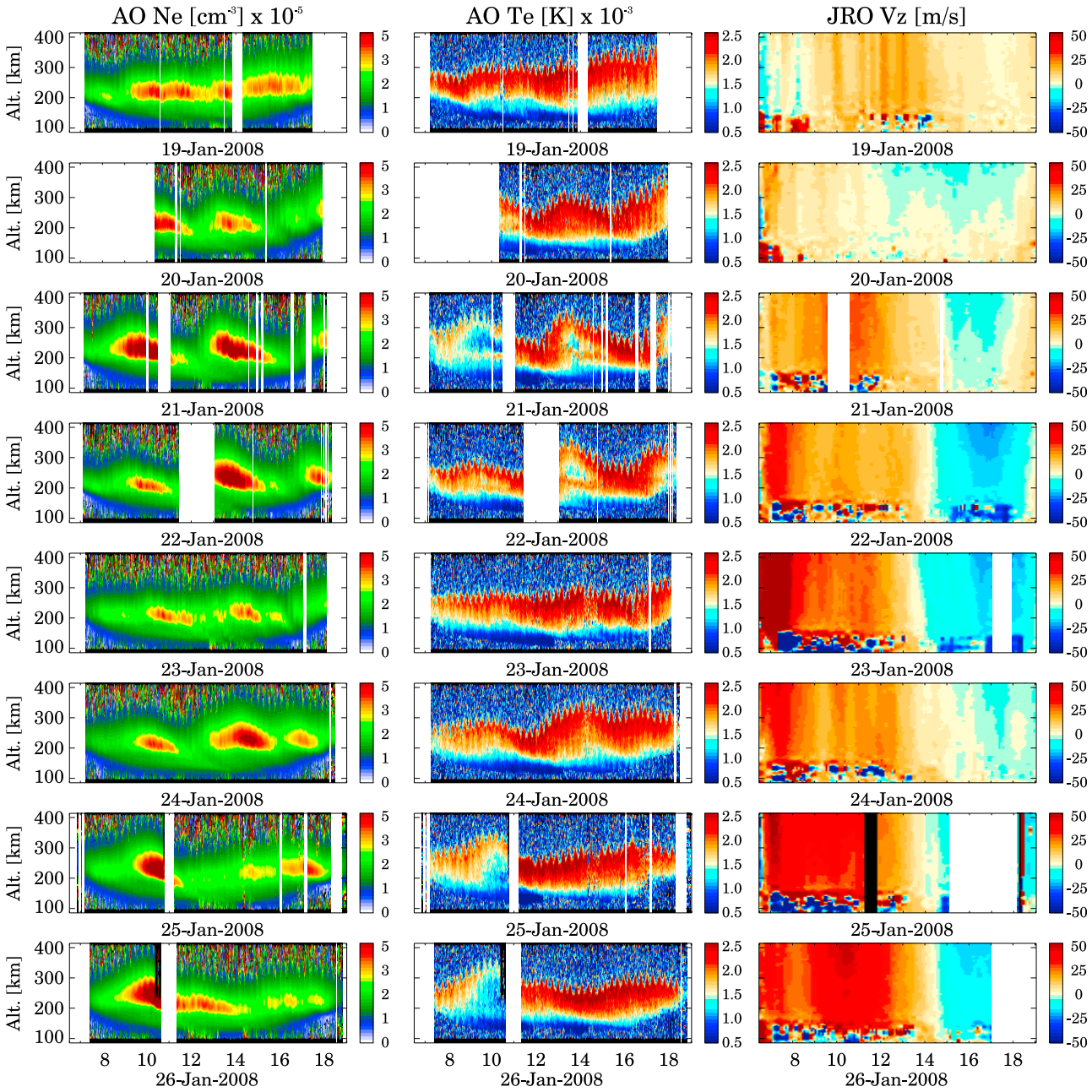


**Figure 2.** Incoherent scatter radar parameters during the January 2008 SSW event: (left) electron density and (middle) electron temperature from the Arecibo Observatory (AO) and (right) vertical drifts from Jicamarca Radio Observatory (JRO). The x axis indicate time in Arecibo local time (i.e., AST) for both AO and JRO.

show the median value obtained from the days before the first SSW warming i.e., before January 21st. Figure 4c shows a TEC map as function of time of the day (*y* axis) and day (*x* axis). The first striking feature is the strong day-to-day variability, particularly taken into account that most of this period has been magnetically quiet and the solar flux has been very low. In addition, we can see that after January 23–24 the TEC shows larger variability and amplitudes. At first look, the strongest perturbations are observed during the daytime hours.

[23] Comparing the TEC results obtained with the ISR data (TECp) (Figure 3) and the relative GPS TEC from Figure 4c, we can see that they are consistent, i.e., both of them show the weak but persistent signature of enhanced TEC right after the first SSW peak (i.e., January 24–27). However, the largest TEC amplitudes are observed several days after.

[24] In Figure 5 we summarize the TEC results by showing the TEC differences (Figure 5a), using the median value of Figure 4 as a reference. In Figure 5b we show the Jicamarca *F*-region drifts differences obtained from the ISR technique (those from Figure 2) and those obtained from the magnetometer $\Delta$H [*Anderson et al.*, 2004]. In this case we use expected quiet time values from the empirical model of

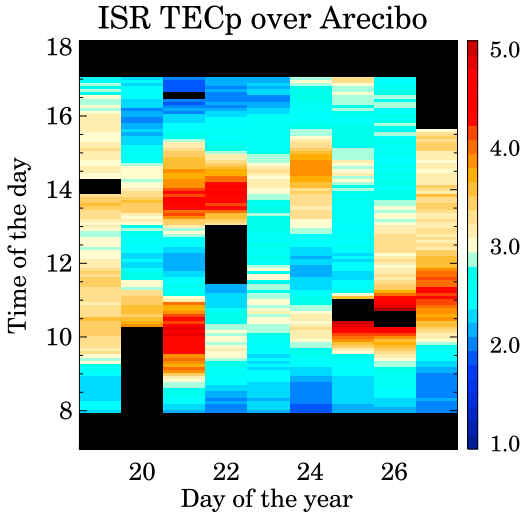


**Figure 3.** Proxy measurements of total electron content (TECp) from integrating the ISR electron density profiles as function of time of the day (AST) (*y* axis) and day (*x* axis). The regions in black represent either no data or bad data (see text for details).

*Scherliess and Fejer* [1999], as a reference. In addition, we show polar stratospheric temperature differences (using the 30-year median value as reference) in black and the daily averaged $K_p$ values (red/blue circles for quiet/active times),

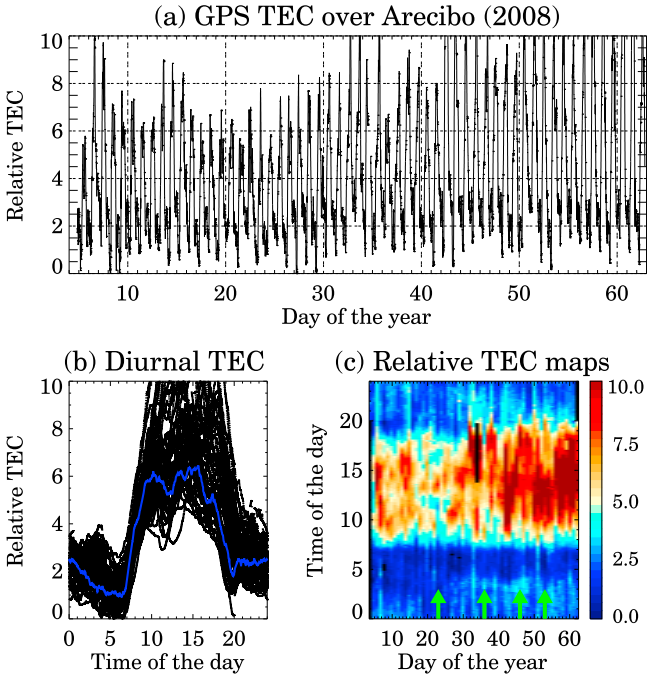


**Figure 4.** Relative TEC measurements from the Arecibo dual-frequency GPS receiver around the January 2008 SSW event: (a) time series, (b) as function of time of the day (AST), and (c) as a function of time of the day and day of the years. The blue solid line in Figure 4b represents the median TEC from all the days before the SSW event. As a reference, the green arrows in Figure 4c represent the times of the SSW.

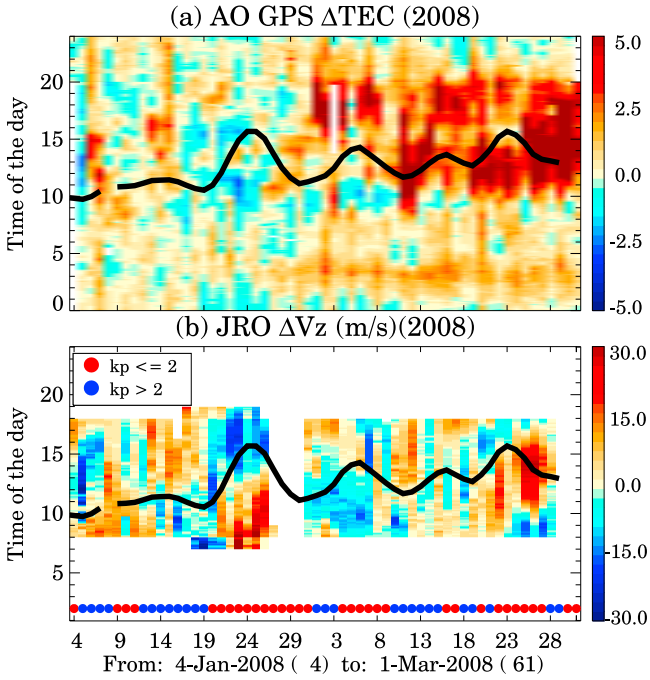


**Figure 5.** (a) AO TEC difference (ΔTEC) using the median values as a reference and (b) JRO vertical drift differences ($\Delta V_z$), both as function of time of the day and day for 2008. The stratospheric polar temperature difference (black solid line) is shown as a reference. The red/blue circles represent magnetically quite/active days.

to put our results in context with these parameters. Note that we are only showing the daytime vertical drifts because: (1) the nighttime ISR values were contaminated by strong coherent echoes due to equatorial spread *F* irregularities, and (2) the magnetometer technique only works during the daytime. Periods of no data are shown in white.

[25] The main features observed in Figure 5 are:

[26] 1. The ΔTEC is much larger a few days after the first warming, particularly during the daytime. Right after the first warming we see a persistent morning enhancement progressing in time as the day increases, but not as large as the later enhancements (Figure 5a).

[27] 2. The equatorial drift differences indeed exhibit an enhanced semidiurnal pattern as reported by *Chau et al.* [2009], particularly during the first warming (Figure 5b).

[28] 3. The largest ΔTEC is observed right after the fourth SSW event. This enhancement is accompanied by a strong drift perturbation in the equator. Again there is a semidiurnal signature in this fourth event, but with a different phase than the first warming, i.e., the positive phase is centered 12–14 AST while during the first warming was around 08–10 AST.

[29] To gain more confidence and understanding on this possible coupling, we also analyzed the 2009 TEC relative values. Figure 6 is similar to Figure 4 but for the January–February 2009 SSW event. Again we observe a very large day-to-day variability (at this point we should say as expected!), and the largest TEC values occur several days after January 24, 2009, i.e., after the peak SSW temperature. Similarly, Figure 7 is in the same format as Figure 5. In this case, instead of the ISR drift values we have used drifts from

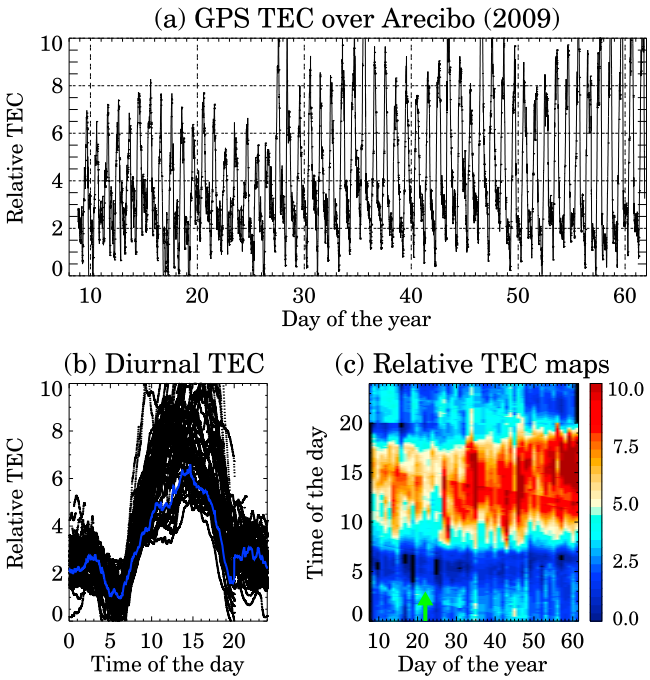


**Figure 6.** Similar to Figure 4 but for 2009.

150-km echoes which are only obtained during the daytime [e.g., *Chau and Woodman*, 2004].

[30] The salient features observed in Figure 7 are:

[31] 1. The ΔTEC is much larger 4–5 days after the peak SSW temperature, particularly during the daytime. This time we can observe that such large differences extend 1–2 hours after local sunset hours (Figure 7a).

[32] 2. The equatorial drift differences exhibit an enhanced semidiurnal pattern that appear to start few days before the stratospheric warming. This time, however, the large amplitude is observed 3–4 days after the peak SSW temperature (Figure 7b).

[33] 3. Although there are many time gaps in the drift data, we can see that the drifts after the SSW present more variability than prior to the warming. Such variability is accompanied by the large ΔTEC values observed over Arecibo.

[34] In the case of 2009, we have also analyzed the foF2 (i.e., *F* region peak densities) values obtained with the ionosonde on site (results not shown here). Doing a similar analysis to the GPS TEC data, we have also observed similar perturbations in foF2 values, i.e., the daytime values after the SSW peak are larger than the values before the SSW peak. However, these perturbations (percentage wise) are lower than the TEC perturbations. Such differences indicate that besides the peak electron density changes, the shape of *F* region also changes.

## 4. Discussion

[35] In this section we first discuss the ISR electron density and temperature observations and then we proceed with the TEC observations over Arecibo. The $\eta_e$ observations from Figure 2 reveal a number of striking differences as compared to the expected behavior for the winter and solar minimum conditions. According to Arecibo data obtained during the period of 1996–2002, the electron density is expected to vary only slightly throughout the day, with minor peaks in the morning hours and afternoon hours [*Lei et al.*, 2007]. From the empirical model of Arecibo ionospheric parameters, daytime peak electron density is expected to be of the order of 5–7 × $10^5$ e/cm$^3$ [*Zhang et al.*, 2005]. This behavior is observed only before the start of the January 2008 SSW event, on January 19, 2008. The observed electron density enhancements and decreases with multiple daytime peaks and valleys, after January 20–21, are thus signs of unusual behavior.

[36] The electron temperature over Arecibo is expected to have two daytime peaks, reaching 1500 K at the *F*-region peak altitudes around 07–08 LT and a stronger peak at 13–15 LT, reaching 1700–1800 K at the *F*-region peak altitudes. In contrast, observations in January 2008 clearly demonstrate a hot, ~2000–2500 K temperature bulge between 200–300 km altitude, which is characteristic for high solar flux conditions [*Lei et al.*, 2007]. The temperature enhancement is followed by a decrease in electron density. This anticorrelation might be explained as follows. An increase in electron density results in the enhancement of electron cooling rate [*Roble*, 1975], leading to the observed daytime decrease in the electron temperature at altitudes around the *F*-region maximum. Since the electron cooling rate is proportional to $\eta_e^2$ and the electron heating rate is proportional to $\eta_e$, dependence of $T_e$ on $\eta_e$ is a complex function resulting from these competing processes. At the Arecibo location and for low levels of electron density, an increase in $\eta_e$ leads to a decrease in $T_e$, as was reported in both observations and simulations [*Goncharenko et al.*, 2005; *Lei et al.*, 2007], while for high levels of electron density the correlation between $\eta_e$ and $T_e$ becomes positive.

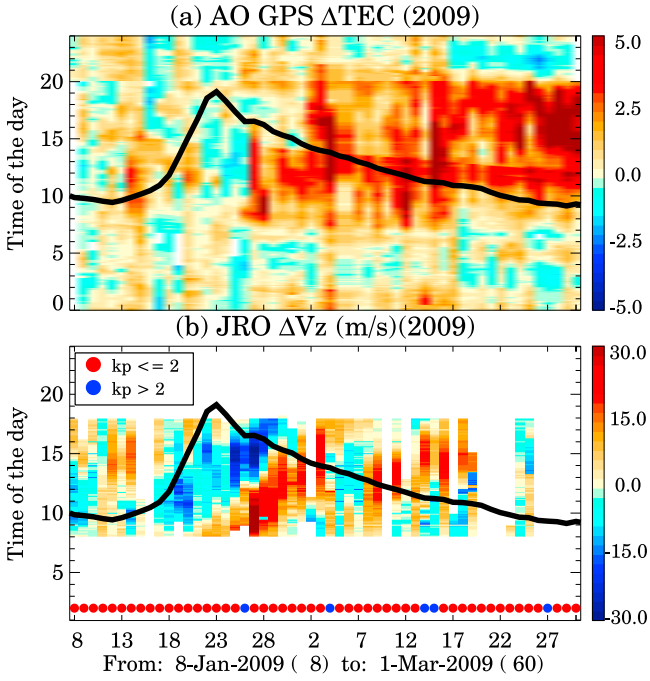


**Figure 7.** Similar to Figure 5 but for 2009. Note that the JRO drift enhancement is delayed 4–5 days with respect to the SSW peak temperature.

In a future work, we are planning to study this anti correlation more carefully and determine its relationship with the ion and neutral temperature, particularly if a longer ISR data set can be obtained. For example how do the ionospheric parameters, besides the TEC, vary during the 4–5 weeks during which the polar stratosphere is usually perturbed?

[37] TIEGCM simulations demonstrate the sensitivity of the ionosphere above Arecibo to the vertical drifts driving the equatorial ionization anomaly [*Lei et al.*, 2007]. When vertical drifts are included in the simulation, the crests of equatorial anomaly move to higher latitudes, resulting in higher electron density above Arecibo. Larger $\eta_e$ also results in stronger electron cooling, leading to lower $T_e$, consistent with the reported observations. We can thus expect that the strong vertical ion drifts observed over Jicamarca, the increase in electron density and the decrease in $T_e$ over Arecibo are part of the same process indicating an increase in low/mid-latitude variability during the SSW events. However the effects over Arecibo, besides the vertical plasma drifts, will depend on other factors that are known to play a role in the strength and location of the equatorial ionization anomaly [e.g., *Hanson and Moffett*, 1966; *Immel et al.*, 2006; *Hagan et al.*, 2007; *Lin et al.*, 2007].

[38] In the case of TEC observations, the ionosphere over Arecibo shows a significant increase of TEC with respect to the days previous to the SSW events, particularly during daytime hours. Again, such TEC increases are accompanied by perturbations in the equatorial vertical drifts observed over Jicamarca. As shown by *Chau et al.* [2009] and *Fejer et al.* [2010], the vertical plasma drifts over Jicamarca present a repetitive and persistent behavior that is highly correlated with SSW events. On the other hand, the response over Arecibo is different from event to event. During the January 2008 event the SSW signature is not as clear as during the fourth warming of the same year. In 2009, the enhanced TEC signature associated with the SSW occurs 4–5 days after the peak SSW temperature. After this warming, the Arecibo ionosphere remained perturbed for a few weeks. Again such perturbations were also associated with anomalous drift patterns observed over Jicamarca.

[39] Recently *Fejer et al.* [2010] has shown that during SSW events, the lunar semidiurnal tides are the ones that get amplified the most. This connection with the lunar tides explains the time delays reported in the January 2009 results (see Figure 7). Briefly, once a SSW has occurred the semidiurnal wave gets amplify right after one of the lunar phases (i.e., either New or Full Moon). In the case of January 2009, the New Moon occurred on January 26, few days after the peak stratospheric polar temperature.

[40] Both events, anomalous equatorial and low latitude ionosphere behavior and SSWs, appear to be caused by the same planetary wave activity. The planetary waves, and in particular the quasi-stationary, do not propagate deep into the ionosphere or to low latitudes due to the presence of critical layers and strong molecular dissipation. On the other hand, the low altitude quasi stationary planetary waves appear to interact nonlinearly with the atmospheric tides. Due to the global nature of the tides, the change resulting from the nonlinear interaction is not confined, and is actually the largest at low latitudes and in the ionospheric *E*-region. These tides in turn modify the *E*-region winds and therefore the electric fields and plasma drifts of the *E*-region dynamo. This hypothesis is supported by a recent numerical modeling work [*Liu et al.*, 2010]. As mentioned above, for the daytime and low solar conditions, the dynamo effects easily modulate the ionospheric low latitude electrodynamics. It is important to note that in this scenario, the planetary wave activity in the mesosphere and lower thermosphere might not be important, and therefore the reduced planetary wave activity reported by *Sathishkumar and Sridharan* [2009] during SSW events do not contradict our results.

[41] Although we report an observational connection and a possible mechanism, we realize that such connection is not very simple to understand. For example, we know that there are other lower atmospheric disturbances besides the planetary waves behind the SSW events (e.g., tides, gravity waves, other planetary waves). Then why do we not see clear evidence of such forcing? The numerical work, like the one done by *Liu et al.* [2010], and more importantly coupled models that self-consistently include the lower atmospheric forcing and the ionosphere electrodynamics, will help in the understanding of this coupling. Moreover, we expect to learn how efficient is indirect coupling via the *E* region dynamo versus the direct coupling of vertically propagating waves, particularly at low and mid latitudes.

## 5. Conclusions

[42] After analyzing two SSW periods, i.e., January–February 2008 and January–February 2009, we are very confident in associating the variability observed in the Arecibo ionosphere with planetary wave activity occurring in the lower atmosphere that causes the SSW events. Moreover, much (if not all) of this connection might be caused indirectly through the *E* region dynamo, particularly when there are larger changes in the equatorial electric fields (and therefore the associated plasma drifts) redistributing plasma to a larger latitudinal range. Our conclusions are supported by the TEC results combined with the equatorial electric fields, namely, the largest TEC perturbations occur during the daytime right after the SSW peak temperatures and they last several days to weeks.

[43] We have observed a strong anticorrelation between the $\eta_e$ and $T_e$. Since we are claiming that during SSW events $\eta_e$ are affected indirectly by changes in the electric fields (plasma drifts) in the *E* region dynamo, then $T_e$, at least during solar minimum conditions, might also be affected indirectly by the *E* region dynamo and therefore by the lower atmospheric forcing.

[44] Finally, our results indicate that any effort towards understanding the low and mid latitude ionosphere weather requires the understanding of the coupling with the lower atmosphere. This understanding is not only important during solar minimum conditions when the effects are easier to observe, but also during solar maximum, where the lower forcing, although subtle, is part of the background conditions.

[45] **Acknowledgments.** JLC thanks the Arecibo Observatory for hosting him as visiting scientist during the preparation of this manuscript. The authors gratefully acknowledge the access to the NCEP data. We also thank A. Anghel for estimating the vertical drifts for the magnetometer data, E. Franco (University of Puerto Rico, Humacao campus) for helping with the processing of the Arecibo TEC data, and A. Coster and W. Rideout for providing the software to get TEC from GPS receivers. The Jicamarca

Radio Observatory is a facility of the Instituto Geofísico del Perú operated with support from the NSF AGS-0905448 through Cornell University. The Arecibo Observatory is part of the National Astronomy and Ionosphere Center, which is operated by Cornell University under a cooperative agreement with the NSF.

[46] Robert Lysak thanks the reviewers for their assistance in evaluating this paper.

## References

Anderson, D., A. Anghel, J. Chau, and O. Veliz (2004), Daytime, vertical E × B drift velocities inferred from ground-based magnetometer observations at low latitudes, *Space Weather*, *2*, S11001, doi:10.1029/2004SW000095.

Bilitza, D., O. Obrou, J. Adeniyi, and O. Oladipo (2004), Variability of fof2 in the equatorial ionosphere, *Adv. Space Res.*, *34*(9), 1901–1906.

Chau, J. L., and R. F. Woodman (2004), Daytime vertical and zonal velocities from 150-km echoes: Their relevance to *F*-region dynamics, *Geophys. Res. Lett.*, *31*, L17801, doi:10.1029/2004GL020800.

Chau, J. L., B. G. Fejer, and L. P. Goncharenko (2009), Quiet variability of equatorial E × B drifts during a sudden stratospheric warming event, *Geophys. Res. Lett.*, *36*, L05101, doi:10.1029/2008GL036785.

Fejer, B. G., and L. Scherliess (2001), On the variability of *F*-region vertical plasma drifts, *J. Atmos. Sol. Terr. Phys.*, *63*, 893–897.

Fejer, B. G., E. R. de Paula, S. A. Gonzalez, and R. F. Woodman (1991), Average vertical and zonal *F* region plasma drifts over Jicamarca, *J. Geophys. Res.*, *96*, 13,901–13,906, doi:10.1029/91JA01171.

Fejer, B. G., M. E. Olson, J. L. Chau, C. Stolle, H. Lühr, L. P. Goncharenko, K. Yumoto, and T. Nagatsuma (2010), Lunar dependent equatorial ionospheric electrodynamic effects during sudden stratospheric warmings, *J. Geophys. Res.*, *115*, A00G03, doi:10.1029/2010JA015273.

Forbes, J. M., S. E. Palo, and X. Zhang (2000), Variability of the ionosphere, *J. Atmos. Sol. Terr. Phys.*, *62*, 685–693.

Forbes, J. M., S. L. Bruinsma, X. Zhang, and J. Oberheide (2009), Surface-exosphere coupling due to thermal tides, *Geophys. Res. Lett.*, *36*, L15812, doi:10.1029/2009GL038748.

Fuller-Rowell, T. J., M. Codrescu, and P. Wilkinson (2000), Quantitative modelling of the ionospheric response to geomagnetic activity, *Ann. Geophys.*, *18*, 766–781.

Goncharenko, L. P., and S. R. Zhang (2008), Ionospheric signatures of sudden stratospheric warming: Ion temperature at middle latitude, *Geophys. Res. Lett.*, *35*, L21103, doi:10.1029/2008GL035684.

Goncharenko, L., J. E. Salah, A. V. Eyken, V. Howells, J. P. Thayer, V. I. Taran, B. Shpynev, Q. Zhou, and J. Chau (2005), Observations of the April 2002 geomagnetic storm by the global network of incoherent scatter radars, *Ann. Geophys.*, *23*, 163–181.

Goncharenko, L. P., J. L. Chau, H.-L. Liu, and A. J. Coster (2010a), Unexpected connections between the stratosphere and ionosphere, *Geophys. Res. Lett.*, *37*, L10101, doi:10.1029/2010GL043125.

Goncharenko, L. P., A. J. Coster, J. L. Chau, and C. E. Valladares (2010b), Impact of sudden stratospheric warmings on equatorial ionization anomaly, *J. Geophys. Res.*, doi:10.1029/2010JA015400, in press.

Hagan, M. E., A. Maute, R. G. Roble, A. D. Richmond, T. J. Immel, and S. L. England (2007), Connections between deep tropical clouds and the Earth's ionosphere, *Geophys. Res. Lett.*, *34*, L20109, doi:10.1029/2007GL030142.

Hanson, W. B., and R. J. Moffett (1966), Ionization transport effects in the equatorial *F* region, *J. Geophys. Res.*, *71*(23), 5559–5572 doi:10.1029/JZ071i023p05559.

Hysell, D. L., J. L. Chau, and J. D. Huba (2009), Topside measurements at Jicamarca during solar minimum, *Ann. Geophys.*, *27*, 427–439.

Immel, T. J., E. Sagawa, S. L. England, S. B. Henderson, M. E. Hagan, S. B. Mende, H. U. Frey, C. M. Swenson, and L. J. Paxton (2006), The control of equatorial ionospheric morphology by atmospheric tides, *Geophys. Res. Lett.*, *33*, L15108, doi:10.1029/2006GL026161.

Lei, J., R. G. Roble, W. Wang, B. A. Emery, and S.-R. Zhang (2007), Electron temperature climatology at Millstone Hill and Arecibo, *J. Geophys. Res.*, *112*, A02302, doi:10.1029/2006JA012041.

Lin, C. H., et al. (2007), Plausible effect of atmospheric tides on the equatorial ionosphere observed by the FORMOSAT-3/COSMIC: Three-dimensional electron density structures, *Geophys. Res. Lett.*, *34*, L11112, doi:10.1029/2007GL029265.

Liu, H.-L., W. Wang, A. D. Richmond, and R. G. Roble (2010), Ionospheric variability due to planetary waves and tides for solar minum conditions, *J. Geophys. Res.*, *115*, A00G01, doi:10.1029/2009JA015188.

MacPherson, B., S. A. González, X. Pi, M. Kelley, G. J. Bailey, M. P. Sulzer, G. Hajj, M. Buonsanto, and C. Wang (2000), Comparison between SUPIM simulations and measured TEC for the January, 1997 storm, *Geophys. Res. Lett.*, *27*, 2845–2848, doi:10.1029/2000GL000026.

Manney, G. L., M. J. Schwartz, K. Krüger, M. L. Santee, S. Pawson, J. N. Lee, W. H. Daffer, R. A. Fuller, and N. J. Livesey (2009), Aura microwave limb sounder observations of dynamics and transport during the record-breaking 2009 arctic stratospheric major warming, *Geophys. Res. Lett.*, *36*, L12815, doi:10.1029/2009GL038586.

Matsuno, T. (1971), A dynamical model of the stratospheric sudden warming, *J. Atmos. Sci.*, *28*, 1479–1494.

Mendillo, M., H. Rishbeth, R. G. Roble, and J. Wroten (2002), Modelling F2-layer seasonal trends and day-to-day variability driven by coupling with the lower atmosphere, *J. Atmos. Sol. Terr. Phys.*, *64*, 1911–1931.

Nicolls, M. J., M. P. Sulzer, N. Aponte, R. Seal, R. Nikoukar, and S. A. González (2006), High-resolution electron temperature measurements using the plasma line asymmetry, *Geophys. Res. Lett.*, *33*, L18107, doi:10.1029/2006GL027222.

Richmond, A. D. (1995), Modeling the equatorial ionospheric electric fields, *J. Atmos. Terr. Phys.*, *57*, 1103–1115.

Rideout, W., and A. Coster (2006), Automated GPS processing for global total electron content data, *GPS Solutions*, *10*, 219–228, doi:10.1007/s10,291–006–0029–5.

Rishbeth, H. (2006), *F* region links with the lower atmosphere?, *J. Atmos. Sol. Terr. Phys.*, *68*, 469–478.

Rishbeth, H., and M. Mendillo (2001), Patterns of F2-layer variability, *J. Atmos. Sol. Terr. Phys.*, *63*, 1661–1680.

Roble, R. G. (1975), The calculated and observed diurnal variation of the ionosphere over Millstone Hill on 23–24 March 1970, *Planet. Space Sci.*, *23*, 1017–1033.

Sathishkumar, S., and S. Sridharan (2009), Planetary and gravity waves in the mesosphere and lower thermosphere region over Tirunelveli (8.7°N, 77.8°E) during stratospheric warming events, *Geophys. Res. Lett.*, *36*, L07806, doi:10.1029/2008GL037081.

Scherliess, L., and B. G. Fejer (1999), Radar and satellite global equatorial *F*-region vertical drift model, *J. Geophys. Res.*, *104*, 6829–6842, doi:10.1029/1999JA900025.

Sridharan, S., S. Sathishkumar, and S. Gurubaran (2009), Variabilities of mesospheric tides and equatorial electrojet strength during major stratospheric warming events, *Ann. Geophys.*, *27*, 4125–4130.

Vineeth, C., T. K. Pant, and R. Sridharan (2009), Equatorial counter electrojets and polar stratospheric sudden warmings—A classical example of high latitude-low latitude coupling?, *Ann. Geophys.*, *27*, 3147–3153.

Zhang, S. R., J. M. Holt, A. P. van Eyken, M. McCready, C. Amory-Mazaudier, S. Fukao, and M. Sulzer (2005), Ionospheric local model and climatology from long-term databases of multiple incoherent scatter radars, *Geophys. Res. Lett.*, *32*, L20102, doi:10.1029/2005GL023603.

Zhao, B., W. Wan, L. Liu, K. Igarashi, M. Nakamura, L. J. Paxton, S.-Y. Su, G. Li, and Z. Ren (2008), Anomalous enhancement of ionospheric electron content in the Asian-Australian region during a geomagnetically quiet day, *J. Geophys. Res.*, *113*, A11302, doi:10.1029/2007JA012987.

N. Aponte, E. Cabassa, S. A. González, and M. P. Sulzer, Arecibo Observatory, HC3 Box 53995, Arecibo, PR 00612.(naponte@naic.edu; edvierc@naic.edu; sixto@naic.edu; msulzer@naic.edu)

J. L. Chau, Radio Observatorio de Jicamarca, Instituto Geofísico del Perú, Apartado 13-0207, Lima, Peru. (jorge.chau@jro.igp.gob.pe)

L. P. Goncharenko, Haystack Observatory, Massachusetts Institute of Technology, Rte. 40, Westford, MA 01886, USA. (lpg@haystack.mit.edu)